



Contents lists available at ScienceDirect

## Pharmacological Research

journal homepage: [www.elsevier.com/locate/yphrs](http://www.elsevier.com/locate/yphrs)

## Perspective

Enalapril treatment discloses an early role of angiotensin II in inflammation- and oxidative stress-related muscle damage in dystrophic mdx mice<sup>☆</sup>Anna Cozzoli<sup>a</sup>, Beatrice Nico<sup>b</sup>, Valeriana Teresa Sblendorio<sup>a</sup>, Roberta Francesca Capogrosso<sup>a</sup>, Maria Maddalena Dinardo<sup>a</sup>, Vito Longo<sup>b</sup>, Sara Gagliardi<sup>c</sup>, Monica Montagnani<sup>c</sup>, Annamaria De Luca<sup>a,\*</sup><sup>a</sup> Unit of Pharmacology, Department of Pharmaco-biology, Faculty of Pharmacy, University of Bari, Italy<sup>b</sup> Department of Human Anatomy and Histology, Faculty of Medicine, University of Bari, Italy<sup>c</sup> Department of Biomedical Sciences and Human Oncology, Faculty of Medicine, University of Bari, Italy

## ARTICLE INFO

**Q1** Article history:  
Received 26 January 2011  
Received in revised form 2 June 2011  
Accepted 2 June 2011

## Keywords:

Muscular dystrophy  
Pre-clinical pharmacological tests  
Angiotensin-II  
Inflammation  
Oxidative stress

## ABSTRACT

Inhibitors of angiotensin converting enzymes (ACE) are clinically used to control cardiomyopathy in patients of Duchenne muscular dystrophy. Various evidences suggest potential usefulness of long-term treatment with ACE inhibitors to reduce advanced fibrosis of dystrophic muscle in the mdx mouse model. However, angiotensin II is known to exert pro-inflammatory and pro-oxidative actions that might contribute to early events of dystrophic muscle degeneration. The present study has been aimed at evaluating the effects of an early treatment with enalapril on the pathology signs of exercised mdx mouse model. The effects of 1 and 5 mg/kg enalapril i.p. for 4–8 weeks have been compared with those of 1 mg/kg  $\alpha$ -methylprednisolone (PDN), as positive control. Enalapril caused a dose-dependent increase in fore limb strength, the highest dose leading to a recovery score similar to that observed with PDN. A dose-dependent reduction of superoxide anion production was observed by dihydroethidium staining in tibialis anterior muscle of enalapril-treated mice, approaching the effect observed with PDN. In parallel, a significant reduction of the activated form of the pro-inflammatory Nuclear Factor- $\kappa$ B has been observed in gastrocnemius muscle. Histologically, 5 mg/kg enalapril reduced the area of muscle necrosis in both gastrocnemius muscle and diaphragm, without significant effect on non-muscle area. In parallel no significant changes have been observed in both muscle TGF- $\beta$ 1 and myonuclei positive to phosphorylated Smad2/3. Myofiber functional indices were also monitored by microelectrodes recordings. A dose-dependent recovery of macroscopic chloride conductance has been observed upon enalapril treatment in EDL muscle, with minor effects being exerted in diaphragm. However a modest effect, if any, was found on mechanical threshold, a functional index of calcium homeostasis. No recovery was observed in creatine kinase and lactate dehydrogenase. Finally the results suggest the ability of enalapril to blunt angiotensin-II dependent activation of pro-inflammatory and pro-oxidant pathways which may be earlier events with respect to the pro-fibrotic ones, and may in part account for both functional impairment and muscle necrosis. The PDN-like profile may corroborate the combined use of the two classes of drugs in DMD patients so to potentiate the beneficial effects at skeletal muscle level, while reducing both spontaneous and PDN-aggravated cardiomyopathy.

© 2011 Published by Elsevier Ltd.

**Abbreviations:** DMD, Duchenne muscular dystrophy; ACE, angiotensin converting enzyme; RAS, renin-angiotensin system; Ang II, angiotensin II; PDN,  $\alpha$ -methylprednisolone; NF- $\kappa$ B, nuclear factor- $\kappa$ B; TGF- $\beta$ 1, transforming growth factor  $\beta$ 1; EDL, extensor digitorum longus; CK, creatine kinase; LDH, lactate dehydrogenase; gCl, sarcolemmal chloride conductance; gK, sarcolemmal potassium conductance; MT, mechanical threshold.

<sup>☆</sup> Perspective articles contain the personal views of the authors who, as experts, reflect on the direction of future research in their field.

\* Corresponding author at: Sezione di Farmacologia, Dipartimento Farmacobiologico, Università degli Studi di Bari "A. Moro", Via Orabona 4, Campus, 70125 Bari, Italy. Tel.: +39 080 5442245; fax: +39 080 5442801.

E-mail address: [adeluca@farmbiol.uniba.it](mailto:adeluca@farmbiol.uniba.it) (A. De Luca).

## 1. Introduction

Duchenne muscular dystrophy (DMD) is a genetic muscle disorder affecting 1 over 3500 male birth and is due to defects of Xp21 gene coding for dystrophin. Animal models do exist, such as the mdx mouse, which are important for pre-clinical studies of pathology mechanisms and therapeutic approaches [1,2]. Dystrophin is a subsarcolemmal protein providing a mechanical link between the intracellular cytoskeleton and the extracellular matrix via the interaction with the dystrophin-associated glycoprotein complex. The absence of dystrophin leads to a progressive muscle fiber death, failing regeneration and fibrosis, through a complex and not fully understood network of events. An early

and chronic inflammatory state plays an important role in degeneration–regeneration events and in the greater susceptibility to oxidative stress; also the absence of dystrophin leads to a dislocalization of nNOS, which contributes to an impaired vasodilatation in contracting muscles and possibly to the loss of calcium homeostasis [3–5]. All these events influence pathology presentation and progression. The absence of dystrophin in cardiac tissue leads to cardiomyocytes death and fibrosis with a clinical picture of cardiomyopathy and late heart failure. Cardiomyopathy is the cause of death in about 10–20% of DMD patients, and requests specific pharmacological management, among which drugs targeting the renin-angiotensin system (RAS) such as angiotensin (Ang)-converting enzyme (ACE) inhibitors [6,7]. Early treatment of DMD boys with perindopril before the onset of cardiac involvement has been found to significantly reduce mortality for both cardiac and non cardiac events, supporting the important therapeutic role of RAS-contrasting drugs [8,9]. Accordingly, multicentric clinical trials in DMD patients with Angiotensin (AT)-1 receptor antagonists vs. ACE inhibitors are upcoming. In addition recent pre-clinical experiments on mdx mice underlined the beneficial effect of captopril vs. the deleterious action of prednisolone on heart function [10]. Inhibition of RAS may also support function and morphology of dystrophic muscle. Cohn et al. [11], have demonstrated that a chronic 6–9 months treatment with losartan, an inhibitor of AT1 receptor of Ang-II, significantly reduces/prevents fibrosis in skeletal muscle of mdx mice. In parallel, contractile function and histological profile were ameliorated. In short term, losartan ameliorates muscle regeneration potential of 9-month-old mdx mice after cardiotoxin injury. These effects have been directly attributed to the inhibition of TGF- $\beta$ 1, the pro-fibrotic cytokine involved in dystrophic muscle fibrosis, due to the documented ability of Ang-II to stimulate TGF- $\beta$ 1 production [12,13]. However, Ang-II may also exert TGF- $\beta$ 1 independent effects that can contribute to fibrosis, to muscle degeneration and to impaired myofiber regeneration [12–14]. In fact Ang-II directly stimulates vasoconstriction and pro-fibrotic Smad signaling and activates, via protein kinase C/NF- $\kappa$ B, the ubiquitin-proteasome pathway; this latter is known to play a role in proteolysis occurring in dystrophic muscle [13–16]. In addition, Ang-II, via receptor-mediated pathways, enhances the activity of NADPH-oxidase, leading to over-production of superoxide anion, the main reactive oxygen species (ROS) produced by the enzyme [17]. The Ang-II induced ROS-dependent signaling may in turn sustain inflammation, reinforcing NF- $\kappa$ B activation and production of pro-inflammatory cytokines [5,17,18]. Interestingly, NADPH-oxidase seems to account for the oxidative stress in heart and muscle of the mdx mouse [19–22], which in turn plays an important role, via NF- $\kappa$ B, in degeneration of dystrophic muscle [4,23,24].

The present research has been focused at evaluating the early role of Ang-II in dystrophic muscle pathology and, consequently, the usefulness of a timely therapy with RAS-contrasting drugs against muscular, other than cardiac, impairment in DMD patients. To this aim we performed a 4–8 weeks treatment with the ACE inhibitor enalapril (1–5 mg/kg), during a stage of mdx pathology (from the 5th to the 12th weeks of age) in which degeneration–regeneration cycles are prominent phenomena with respect to fibrosis. The treatment has been performed in the model of exercised mdx mice, which shows an enhanced mechanical and inflammation-dependent degeneration phase and also in relation to the potential role of RAS in impairing exercise performance [25]. The effects were evaluated with a multidisciplinary approach, on a large array of *in vivo* and *ex vivo* readout parameters and compared with those produced by  $\alpha$ -methyl-prednisolone (PDN), the gold standard for treatment of DMD boys [7].

## 2. Materials and methods

All experiments were conducted in accordance with the Italian Guidelines for the use of laboratory animals, which conform to the European Community Directive published in 1986 (86/609/EEC). Most of the experimental procedures used conform the standard operating procedures for pre-clinical tests in mdx mice available on <http://www.treat-nmd.eu/research/preclinical/SOPs/>.

### 2.1. *In vivo* experiments

#### 2.1.1. Animal groups, treadmill running and drug treatment

A total of 30 mdx male mice of 4–5 weeks of age (Charles River Italy-Jackson Laboratories, USA), and homogeneous for body weight underwent a 30 min running on an horizontal treadmill (Columbus Instruments, USA) at 12 m/min, twice a week (keeping a constant interval of 2–3 days between each trial), for 4–8 weeks, according to standard protocol [19,26]. The reason for using the chronic treadmill exercise and the relative impact on the murine pathology have been extensively described in previous articles [26–29], then minimizing the need of an additional control group of untreated non-exercised mdx mice. Thus the groups were as follows: 8 mdx mice vehicle-treated, 7 mdx mice treated with enalapril at 1 mg/kg, 8 mdx mice treated with enalapril at 5 mg/kg and 7 mdx mice treated with prednisolone at 1 mg/kg. Age and gender-matching wild type mice (wt, C57/BL10ScSn) were also used for specific experimental purposes, as indicated in the text. After reviewing the available information, the two doses of enalapril (Sigma-Aldrich-Italy) were chosen in the medium-high therapeutic range and after proper correction for mouse dosing, so to better correlate with the dose to be used in DMD patients and to avoid false positive/negative [30–32], while the dose of PDN has been chosen based on our previous studies [27,28]. The treatment started one day before the beginning of the exercise protocol, and continued until the day of sacrifice. Each dose of any drug was formulated by proper dilution in sterile water for *i.p.* injection, so to have the desired drug amount in 0.1 ml/10 g body weight. Drug free-animals were injected with equal amount of vehicle. Wild-type mice were left free to move in the cage, without additional exercise and monitored at the same time points of mdx animals, according to the experimental need. Every week all mice were monitored for body weight and fore-limb force by means of a grip strength meter (Columbus Instruments, USA); the end of the 4th week was considered for statistical analysis [19,28]. At this time, an exercise resistance test on treadmill was also performed. All mice were made running on a horizontal treadmill for 5 min at 5 m/min, then increasing the speed of 1 m/min each minute. The total distance run by each mouse until exhaustion was measured [19]. At the end of the 4th week of exercise/treatment the *ex vivo* experiments were also started. Due to the time-consuming nature of some of the *ex vivo* experiments, no more than one–two animals could be sacrificed per day. This required to prolong the experimental time window. Thus, the animals continued to be exercised/treated until the day of sacrifice but no longer than 8 weeks in total.

### 2.2. *Ex vivo* studies

#### 2.2.1. Muscle preparations

Animals of 8–12 weeks belonging to the different groups were anesthetized with 1.2 g/kg urethane *i.p.* Extensor digitorum longus (EDL) muscle of one hind limb and right hemidiaphragm were removed and rapidly placed in the recording chamber for the electrophysiological recordings. Gastrocnemius (GC) muscles from one side were removed and processed for histology procedures, while the contralateral ones were snap frozen in liquid nitrogen and stored at  $-80^{\circ}\text{C}$  until use for biochemical analysis. The same

procedure was used for the left half-side of diaphragm (DIA), while TA muscles were frozen in liquid-nitrogen cooled isopentane for immunofluorescence studies.

### 2.2.2. Electrophysiological recordings by intracellular microelectrodes

EDL muscles and hemidiaphragm strips were bathed at  $30 \pm 1$  °C in the following normal physiological solution (in mM): NaCl 148; KCl 4.5; CaCl<sub>2</sub> 2.0; MgCl<sub>2</sub> 1.0; NaHCO<sub>3</sub> 12.0; NaH<sub>2</sub>PO<sub>4</sub> 0.44 and glucose 5.55, continuously gassed with 95% O<sub>2</sub> and 5% CO<sub>2</sub> (pH = 7.2–7.4).

Two intracellular microelectrode current clamp method was used to measure the membrane electrical properties of muscle fibers, among which membrane resistance (R<sub>m</sub>), according to the cable equation (fiber input resistance of 140 and 200 Ω cm<sup>2</sup>, for EDL and DIA, respectively) [26,28]. The total membrane conductance (gm) was calculated as 1/R<sub>m</sub> in normal physiological solution, while 1/R<sub>m</sub> calculated in a chloride-free solution was the potassium conductance g<sub>K</sub>. Chloride conductance (g<sub>Cl</sub>) was calculated as the mean gm minus the mean g<sub>K</sub> [26,28].

The mechanical threshold (MT) was determined in EDL muscle fibers in the presence of tetrodotoxin (3 μM) using a two microelectrode “point” voltage clamp method [19,28]. In brief, the two microelectrodes (spaced about 50 μm) were inserted into the central region of a superficial fiber, continuously viewed using a stereomicroscope (100× magnification). Depolarizing command pulses of duration ranging from 500 to 5 ms (0.3 Hz) were progressively increased in amplitude from the holding potential (H) of –90 mV until visible contraction. The threshold membrane potential (V<sub>t</sub>, in mV) was read on a digital sample-and-hold millivoltmeter for each fiber at the various pulse durations *t* (in ms); mean values at each *t* allowed the construction of a “strength-duration” curve. Rheobase voltage (R, in mV) and the rate constant (1/τ, s<sup>-1</sup>) to reach the rheobase were obtained by a non-linear least square algorithm using the following equation:  $V = (H - R \exp(t/\tau)) / (1 - \exp(t/\tau))$ , where H is the holding potential (mV), R, is the rheobase (mV) and τ is the time constant. In the fitting algorithm, each point was weighed by the reciprocal of the variance of that mean V and the best fit estimates of the parameters R and τ were made [19,28].

### 2.2.3. Histology and immunohistochemistry

Six–8 μm sections of GC and hemidiaphragm muscles fixed in modified Bouin solution, were stained with toluidin blue which allows to distinguish between healthy myofibres (peripherally nucleated fibers), regenerating/regenerated myofibers, showing central nuclei (centrally nucleated fibers), degenerating fibers, associated to the presence of inflammatory infiltrate, as well as the non muscle tissue (fibrotic or adipose tissue). Morphometric analysis was performed on ten cross-sections from each experimental group by means of at least three animals per group, by

using an Image Analysis software (Olympus Italia, Rozzano, Italy) [27,29]. For immunohistochemistry, GC muscles were fixed in a 4% paraformaldehyde in phosphate-buffered saline (PBS), then washed in PBS, dehydrated in an ascending ethanol series and embedded in paraffin. Coronal sections of 5 μm were collected on polylysine coated slides, deparaffinized, rehydrated and rinsed for 10 min in tris-buffered saline (TBS) pH 7.2. Endogenous peroxidase was blocked by incubation in 3% H<sub>2</sub>O<sub>2</sub> dissolved in methanol for 45 min in the dark. The sections were brought to a boil in 10 mM sodium citrate buffer, pH 6, in the dark for 5 min, and after cooling were treated with 5% horse serum in TBS for 1 h and then sequentially incubated with (i) primaries rabbit anti-phospho-Nuclear Factor(NF)-κB p65 subunit antibody (Cell Signaling Technology, Inc., Celbio Italia) and with goat phospho-Smad2/3(Ser 423/425) (Santa Cruz Biotechnology, Inc.) [29] both diluted 1:50 in TBS overnight at 4 °C; (ii) secondary antibody, biotin-labeled swine anti-rabbit IgG and biotin-labeled swine anti goat (Vector Inc., Burlingame, CA) followed by streptavidin-peroxidase conjugate (Vector Inc.). The developing reaction was performed in 0.05 M acetate buffer pH 5.1, 0.02% 3-amino-9-ethylcarbazole grade II (Sigma Chemical Co.), and 0.05% H<sub>2</sub>O<sub>2</sub>. Sections were then washed in the same buffer, counterstained with Mayer's hematoxylin for 1 min and mounted in buffered glycerin. Negative controls, obtained by substituting normal rabbit serum and normal goat for the primaries antibodies, showed no staining of the sections.

Dihydroethidium (DHE; Molecular Probes Inc., USA) was used to evaluate superoxide (O<sub>2</sub><sup>-</sup>) production in muscles *in situ* [19,22]. DHE freely enters cells where, in the presence of O<sub>2</sub><sup>-</sup>, it is oxidized to ethidium bromide that intercalates within nuclear DNA and emits red fluorescence in proportion to the amount of O<sub>2</sub><sup>-</sup> present (excitation at 488 nm, emission at 610 nm). Unfixed, frozen TA muscles were cut into 10-μm-thick cross-sections. Sections were pre-hydrated with PBS (10 min) and then incubated with DHE (2 μM, 30 min, 37 °C) in a dark, humidified chamber. Sections were subsequently washed, stained with 4,6-diamidin-2-phenylindol dichlorohydrate (DAPI, Santa Cruz Biotech, Inc., California, USA) to visualize cell nuclei, and mounted on a coverslip. Results were observed with an epifluorescent Zeiss Axiovert TS100 microscope with appropriate filters. Images were captured with a CCD camera in conjunction with AxioVision Software (Zeiss) using identical imaging settings for each image acquisition. Densitometric analysis for merging of DHE and DAPI fluorescence was performed using AxioVision Rel 4.6.3 software. Fluorescence was quantified by counting the number of pixels in identical fields for each group and expressed as relative increase with respect to unitary value from wt mice [19].

### 2.2.4. Determination of transforming growth factor-β1 (TGF-β1)

TGF-β1 protein was measured by enzyme-linked immunosorbent assay (ELISA), according to the manufacturer's instructions

**Table 1**  
Effect of enalapril treatment on body weight and fore limb muscle strength of mdx mice.

Groups	BW T0	BW T4	ΔBW (T4–T0)	F <sub>max</sub> T0	F <sub>max</sub> T4	ΔF <sub>max</sub> (T4–T0)	NF T0	NF T4
WT (5)	19.7 ± 0.41	25.41 ± 0.8	5.7 ± 0.71	0.122 ± 0.006	0.181 ± 0.01	0.058 ± 0.018	6.25 ± 0.4	7.09 ± 0.33
Mdx + vehicle (8)	17.8 ± 1.24	22.3 ± 1.36*	4.48 ± 0.35	0.113 ± 0.01	0.143 ± 0.01*	0.03 ± 0.009	6.29 ± 0.25	6.33 ± 0.34
Mdx + Enal 1 (7)	16.0 ± 0.71*	20.8 ± 0.57*	4.86 ± 0.54	0.106 ± 0.009	0.148 ± 0.004*	0.042 ± 0.006	6.62 ± 0.49	7.15 ± 0.26
Mdx + Enal 5 (8)	18.8 ± 0.72	22.8 ± 0.59*	4.05 ± 0.77	0.122 ± 0.008	0.176 ± 0.004 <sup>#</sup>	0.054 ± 0.007 <sup>§</sup>	6.49 ± 0.28	7.77 ± 0.22 <sup>§</sup>
Mdx + PDN (7)	19.9 ± 0.99	23.3 ± 0.31	3.44 ± 0.88	0.107 ± 0.01	0.160 ± 0.01	0.050 ± 0.01	5.32 ± 0.38	6.86 ± 0.35 <sup>§</sup>

Columns are as follows: Groups of mice used (in brackets the number of mice per group); wild type C57BL10 (WT); untreated mdx mice (Mdx + vehicle); Mdx mice treated with enalapril 1 mg/kg (Mdx + Enal 1); Mdx mice treated with enalapril 5 mg/kg (Mdx + Enal 5); Mdx mice treated with α-methylprednisolone (Mdx + PDN); body weight, in g at the beginning (T0) and at the end of 4-week-protocol (T4); ΔBW, difference between body weights at T4 and T0; F<sub>max</sub>, maximal fore limb strength, in kg at either the beginning (T0) and at the end of 4-week-protocol (T4); ΔF<sub>max</sub>: fore limb strength increment between T4 and T0. NF: fore limb strength normalized to body weight at either the beginning (T0) and at the end of 4-week-protocol (T4). Each value is the mean ± S.E.M. For each parameter, the statistical significance between groups was evaluated by ANOVA test for multiple comparison (F values) and Bonferroni's *t*-test post hoc correction. Significance at ANOVA test was found for the following parameters BW (F > 3; p < 0.04); F<sub>max</sub> at T4 (F > 3; p < 0.05); NF at T4 (F > 4; p < 0.01). The Bonferroni's test showed statistical significance as shown in the table with respect to the following groups: \*WT (0.002 < p < 0.04); <sup>§</sup>Mdx + vehicle (0.002 < p < 0.01), <sup>#</sup>Mdx + Enalapril 1 mg/kg (p < 0.01).

(R&D System, Minneapolis, MN, USA). Briefly, 10–20 mg of tissue was homogenized in 500  $\mu$ l of a solution containing 1% Triton X-100, 20 mM Tris pH 8.0, 137 mM sodium chloride, 10% glycerol, 5 mM ethylenediaminetetraacetic acid and 1 mM phenylmethylsulphonyl fluoride [26]. TGF- $\beta$ 1 levels were expressed as pg of TGF- $\beta$ 1/ $\mu$ g of total protein, measured by classical Bradford analysis.

### 2.2.5. Creatine kinase and lactate dehydrogenase in plasma and/or blood

Blood was collected by heart puncture soon after animal death in EDTA/heparin rinsed centrifuged tubes. The blood was centrifuged at 3000  $\times$  g for 10 min and plasma was separated and immediately used or stored at  $-20^{\circ}$ C for less than one week. Creatine kinase and

lactate dehydrogenase determinations were performed by standard spectrophotometric analysis by using diagnostic kits (Sentinel, Farmalab, Italy) [27].

### 2.3. Statistics

All data is expressed as mean  $\pm$  standard error of the mean (S.E.M.) or  $\pm$  standard deviation (S.D.). The S.E. estimate for the fitted rheobase (R) values (and relative statistical analysis) were obtained as previously described [28]. The size of the S.E. of normalized strength increment ( $\Delta$ NF) has been calculated from the standard error of the mean (S.E.M.) values of normalized strength at each time, taking into account the size, as percent of the mean, of each S.E.M. and considering the sum of them as indicative of the maximal size of the calculated S.E. This approach allowed to minimize the unpredictable variability due to differences in absolute values of the individual differences [33]. Statistical analysis for direct comparison between two means was performed by unpaired Student's *t* test. Multiple statistical comparisons between groups, were performed by one-way ANOVA, with Bonferroni's *t* test post hoc correction for allowing a better evaluation of intra- and inter-group variability and avoiding false positive. Pathology-related alterations in mdx groups were detected as the amount of significant impairment with respect to wt mice. The recovery score by the drug treatment, as percentage of change toward the wt value, has been evaluated according to the Standard Operating Procedures described in the Treat-NMD web site ([http://www.treat-nmd.eu/research/preclinical/DMD\\_SOPs](http://www.treat-nmd.eu/research/preclinical/DMD_SOPs)).

## 3. Results and discussion

### 3.1. Effect of enalapril on forelimb strength and resistance to treadmill exercise

The body weight values at the beginning and at the end of the in vivo phase, along with the 4-week increments, are shown in Table 1. As can be seen, no significant changes have been observed in the increment over time in the various experimental groups, although a slightly lower increment has been observed in enalapril 5 mg/kg and in the PDN-treated groups. A less increment in body

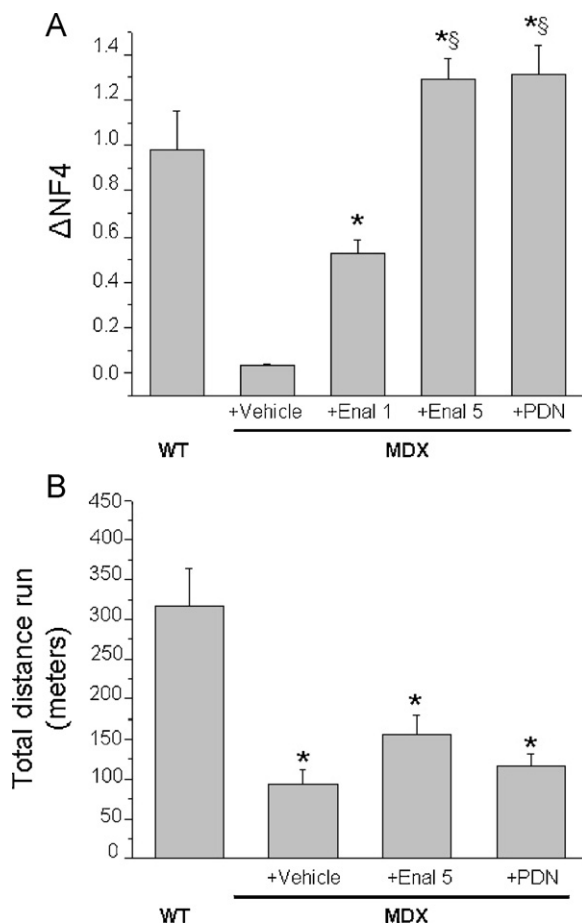


**Fig. 1.** Effect of enalapril treatment on fore limb strength and resistance to exercise of mdx mice. (A) The bars show the normalized force increment ( $\Delta$  normalized force) for wild type (WT) and mdx mice either untreated (vehicle) or treated with enalapril 1 mg/kg (Enal 1), 5 mg/kg (Enal 5) or  $\alpha$ -methylprednisolone 1 mg/kg (PDN).  $\Delta$  normalized force has been calculated as follows: for each mouse the fore limb strength has been normalized to the respective body weight both at the beginning of exercise/treatment protocol (Time 0) and after 4 weeks (Time 4). The difference between the normalized strength values at the two time points allowed to calculate for each mouse of each group the increment and to evaluate the effect of either exercise, treatment or both on it. Each bar is the mean  $\pm$  S.E. (see Section 2) from the number of mice in brackets above each bar. Statistical significance between groups was evaluated by ANOVA test for multiple comparison and Bonferroni *t*-test post hoc correction and was as follows:  $F > 38$ ;  $p < 0.0001$ ;  $10 < F < 40$ ;  $p < 0.005$ ; significantly different with respect to \*vehicle-treated mdx ( $p < 0.0001$ ); §enalapril 1 mg/kg treated mice ( $p < 0.0001$ ). Although not shown in the figure, the values from mdx mouse groups were significantly different with respect to those of WT mice. In (B) is shown the total distance (in m) run by wt and mdx mice treated or not with enalapril 5 mg/kg (Enal 5) or  $\alpha$ -methylprednisolone 1 mg/kg (PDN) in an exhausting test on treadmill. Each bar is the mean  $\pm$  S.E.M. from 5 to 6 animals. Statistical significance between groups was evaluated by ANOVA test for multiple comparison (*F* values) and Bonferroni *t*-test post hoc correction and was as follows:  $F = 11.03$ ;  $p < 0.0005$ ; \*significantly different with respect to WT mice ( $p < 0.005$ ).

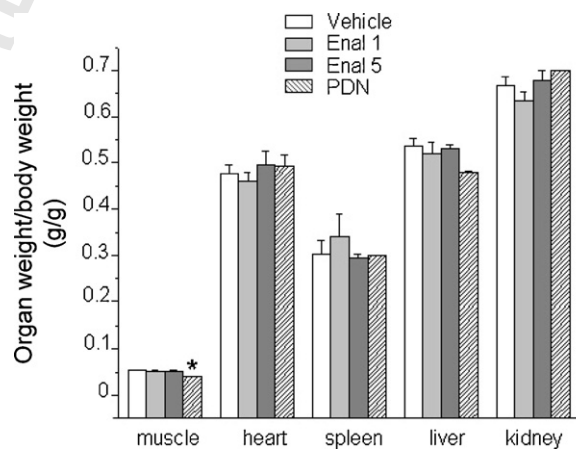


**Fig. 2.** Effect of drug treatment on weight of organs of mdx mice. The figure shows the weight of EDL muscle, heart, spleen, liver and kidney of mdx mice either untreated (vehicle) or treated with enalapril 1 mg/kg (Enal 1), 5 mg/kg (Enal 5) or  $\alpha$ -methylprednisolone 1 mg/kg (PDN). Each bar is the mean  $\pm$  S.E.M. from 5 to 8 animals and show the organ values normalized with respect to the individual body weight. When S.E.M. not visible is because lower than scale resolution. The normalized values for the liver have been scaled by a factor of ten for graphical reasons. ANOVA analysis and Bonferroni's *t* test showed statistical differences only for muscle weight ( $F = 4.7$ ;  $p < 0.01$ ) \*significantly different vs. mdx vehicle-treated ( $p < 0.002$ ).

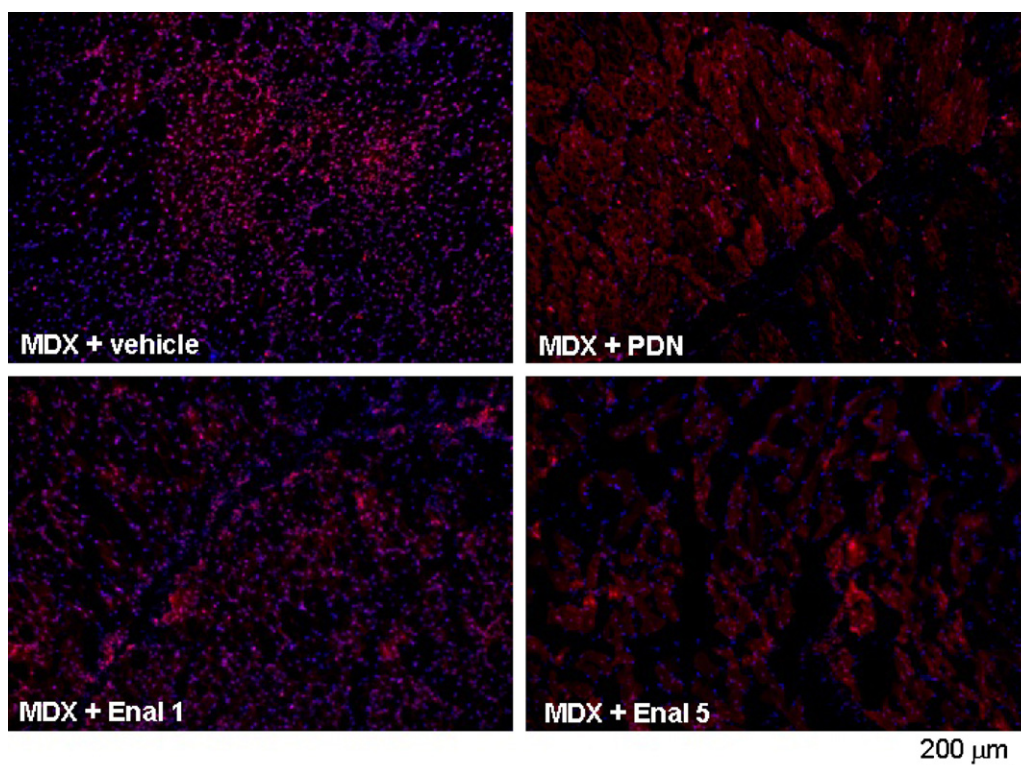


**Fig. 3.** Effect of drug treatment on superoxide production in TA muscle of mdx mice. *In situ* detection of  $O_2^-$  in TA muscles was performed by visualizing red fluorescence in cell nuclei of tissue sections loaded with DHE as described under Section 2. Representative fluorescent photomicrographs from independent sets of experiments are shown for TA muscle cross-sections at 10 $\times$  magnification. Merging (magenta fluorescence) of DHE (red fluorescence) and DAPI (blue fluorescence) staining is indicative of  $O_2^-$  production in cell nuclei from mdx mice either untreated (MDX + vehicle), or treated with  $\alpha$ -methylprednisolone 1 mg/kg (MDX + PDN), enalapril 1 mg/kg (MDX + Enal 1) or enalapril 5 mg/kg (MDX + Enal 5). (For interpretation of the references to color in this figure legend, the reader is referred to the web version of the article.)

weight with PDN has been also observed in other studies [27]. The mdx groups showed slight but not significantly lower values of fore limb strength with respect to wt animals at the beginning of the experimental protocol. In line with previous observations, the maximal grip strength was significantly lower after 4 weeks of protocol in the vehicle-treated mdx animals with respect to wt animals. The treatment with enalapril was protective, with a clear dose-dependent effect on both the absolute value and its 4-week increment (Table 1). On this latter the recovery score was 42% and 85% with 1 mg/kg and 5 mg/kg of enalapril, respectively. A similar protection has been observed with 1 mg/kg PDN (71%). In order to take into account the inter-individual influence of body weight, the forelimb strength values were normalized to body weight both at the beginning (time 0) and after 4 weeks (time 4) (Table 1). The normalized force increment for each mouse over the 4 weeks was then calculated as the difference (normalized force T4) – (normalized force T0) (Fig. 1A). Again, a clear dose-dependent increase in normalized strength increment by enalapril was observed; both enalapril at 5 mg/kg and PDN showed increments in normalized values even higher than that observed in wt mice. To investigate further on the degree of functional amelioration by the drugs, an acute test of resistance to treadmill exercise was performed at the end of the *in vivo* phase. As shown in Fig. 1B, the mdx mice were significantly less resistant to exercise with respect to wt. No significant improvement in this parameter has been observed in both enalapril and PDN treated mdx mice, although the enalapril-treated mice run for a greater distance with respect to the other two groups. *In vivo* fatigability of dystrophic animals is considered due to impaired nitric-oxide dependent vasodilatation [34]; the present results suggest a partial role of Ang II-related vasoconstriction in poor exercise-resistance of mdx mice. Also, the results do not support a role of RAS in the poor exercise performance of mdx animals [25].

Apart from a decrease in PDN-treated group, no significant differences were found in the weight of fast-twitch EDL muscle between the experimental groups. Similarly, no significant differences were found in the weight of vital organs (liver, kidney, heart and spleen) (Fig. 2), suggesting no gross toxic effects due to the treatments.

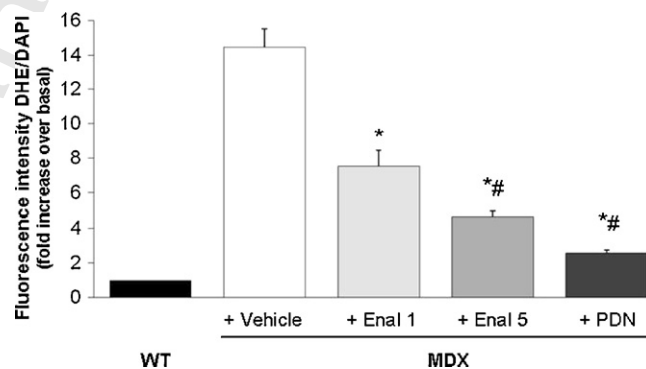


**Fig. 4.** Effect of drug treatment on densitometric determination of superoxide anion production. Densitometric determination of DHE fluorescence in the nuclei of TA muscles from mdx mice treated or not with either enalapril at 1 (Enal 1) and 5 mg/kg (Enal 5) or  $\alpha$ -methyl prednisolone (PDN) is shown. Each bar is the mean  $\pm$  S.E.M. of the value of fluorescence relative to the merging of DHE (red) and DAPI (blue) staining of wt (arbitrarily considered as unitary) from analysis of 5–16 fields and 3–5 muscle per group (at 40 $\times$  magnification). A significant difference among groups was found by ANOVA analysis ( $F=35.57$ ;  $p<0.0001$ ), Bonferroni post hoc *t*-test for individual differences between groups are as follows: significantly different \*vs. vehicle-treated mdx ( $p<0.0001$ ) and #vs. enalapril 1 mg/kg treated mdx group ( $p<0.05$ ).

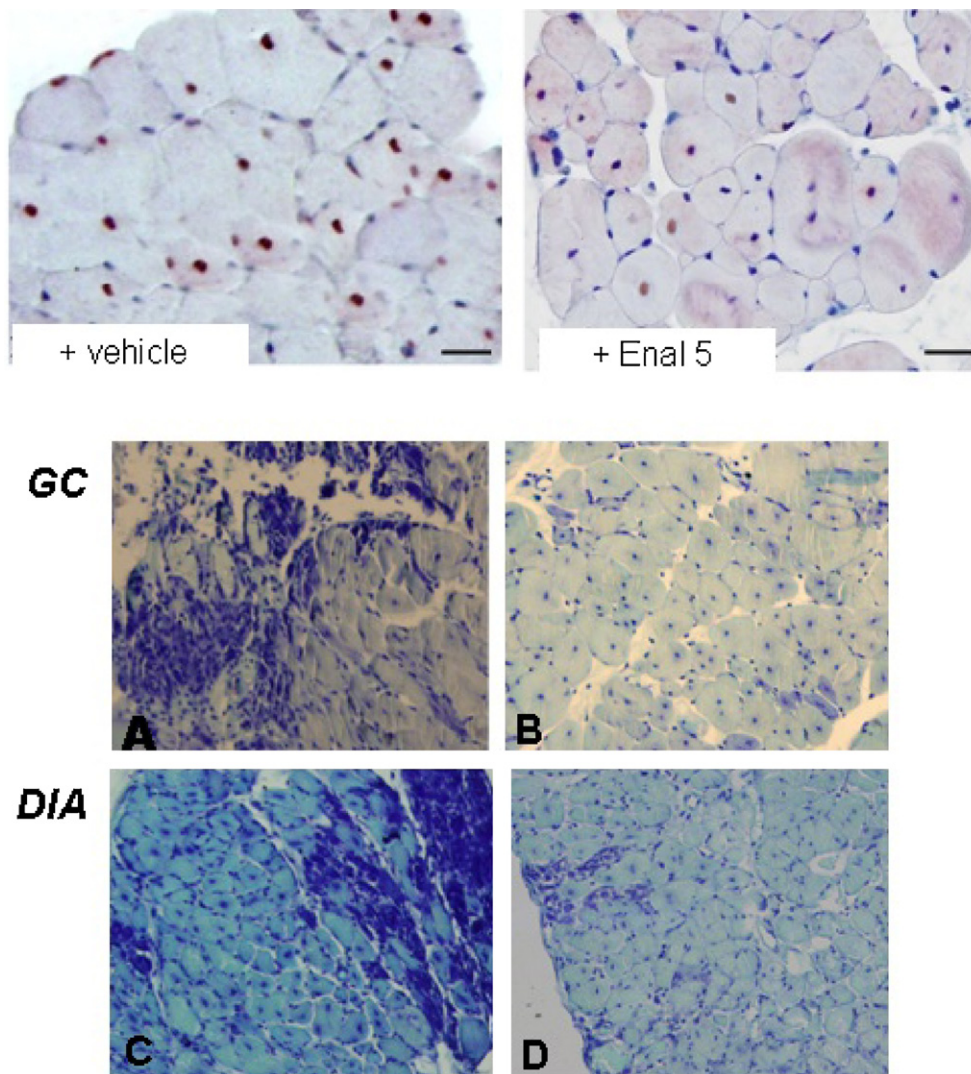


**Fig. 5.** Effect of enalapril treatment on activated NF-kB-positive myofibers and histological profile of mdx mouse muscles. Upper panel: immunohistochemical expression of anti p65-phospho-NF-kB in gastrocnemius muscle fibers of mdx mice either untreated (+ vehicle) and treated with enalapril 5 mg/kg (+ Enal 5). The mdx muscle shows numerous positive nuclei in the peripherally and centronucleated fibers, while enalapril-treated muscle show a reduced number of NF-kB labeled nuclei, mostly located in the centronucleated fibers. Scale bar, 33.3  $\mu$ m. Lower panel: Morphological features of gastrocnemius (GC) and diaphragm (DIA) muscles from untreated (A and C) and enalapril 5 mg/kg treated (B and D) mdx mice, by toluidine blue staining. The sections from untreated exercised muscles showed a less homogenous structure, with greater variability in fiber dimension, larger areas of necrosis accompanied by mononuclear infiltrates and/or small regenerating fibers. A areas of non muscle tissue are also present. Enalapril treated muscles showed a more homogenous architecture with less area of necrosis. Pictures at 20 $\times$  magnification.

### 3.2. Effect of Enalapril on markers of oxidative stress and inflammation

Enalapril acts by contrasting the effects of Ang-II, which is claimed to exert pro-oxidant and pro-inflammatory actions in skeletal muscle. In particular, Ang-II activates NADPH oxidase with

the production of superoxide anion [17]. Importantly, an overexpression of the muscular isoform of the NADPH oxidase, NOX2, and an increased level of superoxide anion do occur in dystrophic muscles [19–21]. In order to evaluate the potential anti-oxidant effect of enalapril, we tested the ROS-sensitive dye DHE on tibialis anterior (TA) muscle. The specific fluorescence was evaluated by

**Table 2**  
Effect of Enalapril treatment on histology profile of diaphragm and gastrocnemius muscle of mdx mice.

	% NF	% CNF	Area NF ( $\mu^2$ )	Area CNF ( $\mu^2$ )	% necrotic area	% non-muscle area
GC Mdx vehicle	28 $\pm$ 6.6	74 $\pm$ 7	832 $\pm$ 138	1757 $\pm$ 453	5.7 $\pm$ 1.9	9.6 $\pm$ 3.2
GC Mdx + Enalapril	33 $\pm$ 2*	67 $\pm$ 6*	1141 $\pm$ 543	1496 $\pm$ 316	1.2 $\pm$ 0.2 <sup>§</sup>	7.4 $\pm$ 4.6
DIA Mdx vehicle	52 $\pm$ 6	48 $\pm$ 6	699 $\pm$ 55	1292 $\pm$ 219	8.1 $\pm$ 4.7	7.1 $\pm$ 3.5
DIA Mdx + Enalapril	46 $\pm$ 16	54 $\pm$ 4*	830 $\pm$ 108*	1598 $\pm$ 226*	1.8 $\pm$ 0.7**	5.3 $\pm$ 2.4

The columns from left to right show the mean values  $\pm$  S.D. obtained from at least 9 sections from 3 preparations from each experimental group. % NF, is the percent of the normal fibers while % CNF is the percent of centronucleated fibers, i.e. regenerated fiber which replace normal peripherally nucleated fibers and are an index of degeneration-regeneration cycles in the muscle. Area of both normal fibers (NF) and centronucleated fibers (CNF). The % of necrotic area, is the area composed of necrotic fibers with a large infiltration of inflammatory mononucleated cells, while the % percent of non-muscle area, represents the area of space between fibers or between groups of muscle fibers that is not stained as muscular tissue and is composed by connective and/or adipose tissue. Significantly different by unpaired Student's *t* test for \**p* < 0.05, \*\**p* < 0.001 and <sup>§</sup>*p* < 0.0001 vs. muscle-related vehicle-treated mdx group.

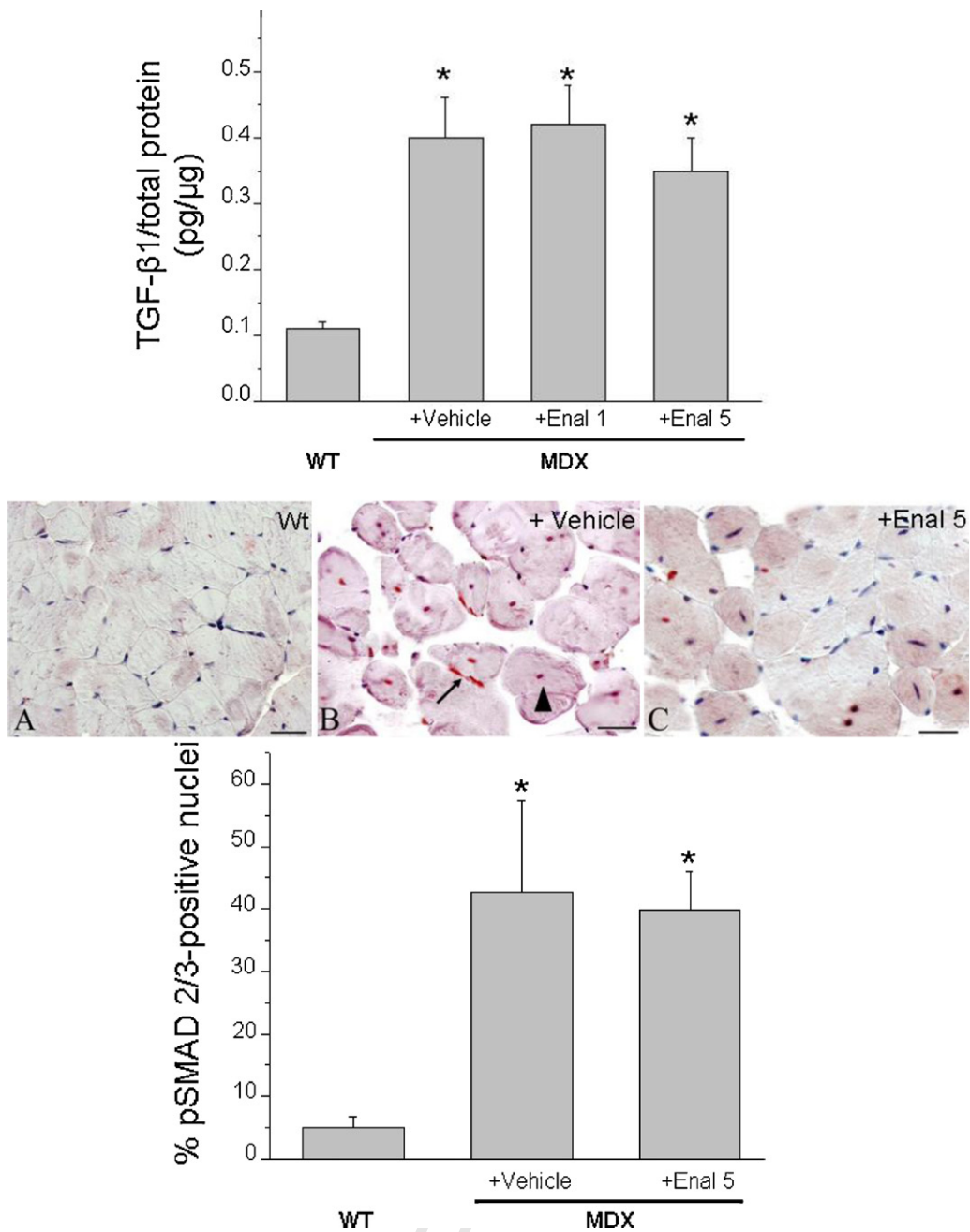


**Fig. 6.** Effect of enalapril treatment on pro-fibrotic signaling in mdx mouse muscles. The bars in the upper panel show the levels of total TGF-β1 in gastrocnemius muscle, measured by ELISA. Each value is the mean ± S.E.M. from 5 to 9 preparations. Statistical significance has been evaluated by ANOVA and Bonferroni's *t* test post hoc correction and was as follows  $F > 10$ ;  $p < 0.0001$ . \*Significantly different with respect to WT ( $p < 0.0001$ ). The middle panel shows representative immunohistochemical expression of p-Smad2/3 in gastrocnemius muscles fibers of wt (A), exercised mdx (B) and enalapril (5 mg/kg) treated exercised mdx (C) mice. No labeling of the nuclei and fibers is present in wt muscle (A), while the mdx muscle shows numerous positive nuclei in the peripherally (B, arrow) and centronucleated fibers (B, arrowhead). Enalapril-treated mice (C) show a general trend toward a reduced number of p-Smad2/3 labeled nuclei (scale bar, 33.3 μm). The quantitative estimation of positive myonuclei is represented in the lower panel. The analysis (at least 3 animals/group and 9 fields/muscle; mean ± S.D.) showed only a slight not significant decrease in pSmad2/3 reactivity in enalapril-treated group vs. vehicle treated one. Statistical significance has been evaluated by ANOVA and Bonferroni's *t* test post hoc correction and was as follows  $F > 7$ ;  $p < 0.03$ ; \*significantly different with respect to WT ( $p < 0.02$ ).

the magenta merging of DAPI and DHE signals, indicating the specific DNA binding of  $O_2^-$  activated dye. In line with previous data [19], a widespread and intense nuclear staining was observed in mdx muscles (Fig. 3). Reactivity was observed in both myonuclei and in nuclei of non-muscle cells, likely inflammatory infiltrates. A marked reduction of staining has been observed with both enalapril 5 mg/kg and PDN 1 mg/kg. The densitometric analysis clearly evidenced a significant and dose-dependent reduction of reactivity toward the wildtype condition in the enalapril-treated animals (Fig. 4). The effect by 5 mg/kg enalapril approached that observed

with PDN, suggesting a control of ROS production by enalapril similar to that exerted by a classical anti-inflammatory approach (Fig. 4). By the way, this is also the first experimental proof that PDN in fact reduces ROS production in dystrophic muscle.

ROS are main signals for NF-κB activation and this latter is a pro-inflammatory transcription factor claimed to have a key role in muscular dystrophy [23,24]. Then, we performed an immunostaining for the phosphorylated NF-κB p65 subunit, the activated form that undergoes nuclear translocation. In line with previous findings [29], a high percentage of fibers positive for activated NF-κB was

found in GC muscle of vehicle-treated mdx mice ( $60 \pm 7\%$ ;  $N = 3/9$ ). Interestingly, a marked and significant reduction of positive nuclei was observed in enalapril-treated GC mdx muscles. In fact the positivity was observed in only  $28 \pm 13.5\%$  of fibers in the 5 mg/kg treated group (mean  $\pm$  SD;  $p < 0.05$  by Student's *t* test) (Fig. 5 upper panel).

### 3.3. Effect enalapril on histopathology and biochemical markers

The GC and DIA muscles of vehicle-treated mdx mice showed remarkable morphological alterations with extensive areas of necrosis, and a wide presence of centronucleated fibers, as a clear index of degeneration-regeneration cycles. The architecture was markedly compromised due to irregular fiber shape and to the presence of cluster of small regenerating fibers, of mononuclear infiltrates and of areas of non-muscle tissue (Fig. 5 - lower panel A, B).

The treatment with enalapril led to an amelioration of the histological picture in both muscles, in term of a more regular tissue architecture and significant reduction of damaged areas vs. untreated ones (Fig. 5 lower panel C, D). In both muscles, the morphometric analysis showed a significant decrease of the area of necrosis (Table 2). The decrease in necrosis was similar to the 50-80% decrease observed in both muscles after PDN treatment (data not shown). In GC muscle an increase in the percent of normal peripherally nucleated fibers vs. centronucleated ones was observed, supporting a decrease in the degeneration-regeneration cycles. This was corroborated by the observation that centronucleated fibers in enalapril-treated GC muscle also showed a trend toward smaller area, while the opposite was observed in normal fibers (Table 2). Interestingly, in diaphragm, the decrease of necrosis was accompanied by an increase in centronucleated fibers; in parallel a significant increase of the area of both normal and centronucleated fibers was observed (Table 2). This suggests a possible role of enalapril in reducing degeneration meanwhile enhancing regeneration efficiency in a muscle-type specific manner. In both muscles, the area covered by non-muscle tissue, and likely related to fibrosis was only slightly but not significantly reduced, suggesting minor effects of enalapril on pro-fibrotic pathways. To verify this hypothesis, the total level of TGF- $\beta$ 1 has been measured by ELISA assay. As can be seen in Fig. 6 (upper panel), no significant changes were found in the levels of TGF- $\beta$ 1 in GC muscle of mdx mice treated with enalapril at either dosages. Similarly, in diaphragm the TGF- $\beta$ 1 level were  $0.46 \pm 0.06$  pg/ $\mu$ g

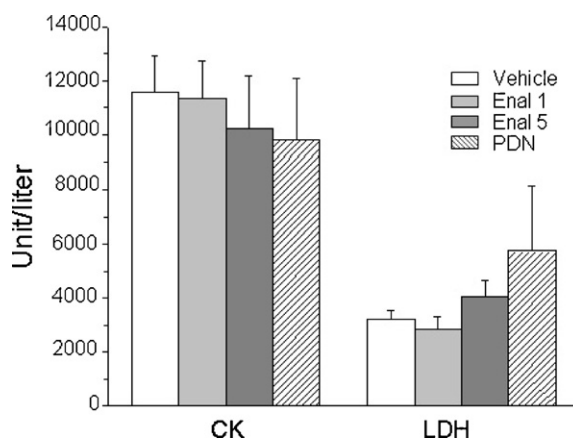


**Fig. 7.** Effect of enalapril treatment on plasma level of creatine kinase and lactate dehydrogenase of mdx mice. Plasma level of creatine kinase (CK) and lactate dehydrogenase (LDH) measured by standard spectrophotometric analysis. Each column is the mean  $\pm$  S.E.M. from 5 to 8 animals. No significant statistical differences were observed between values of mdx mice (either treated or not).

( $n = 9$ ) and  $0.43 \pm 0.1$  pg/ $\mu$ g ( $n = 5$ ) in vehicle and 5 mg/kg treated enalapril, respectively. In order to better evaluate the effect of enalapril on pro-fibrotic signaling, the percentage of myonuclei positive to activated phosphorylated Smad2/3 was estimated in GC muscles. While almost no reactivity has been detected in wt GC muscle, vehicle treated mdx myofibers showed an extensive reactivity occurring in both central (by 63%) and peripheral nuclei (by 37%). The reactivity was generally less evident in GC muscles

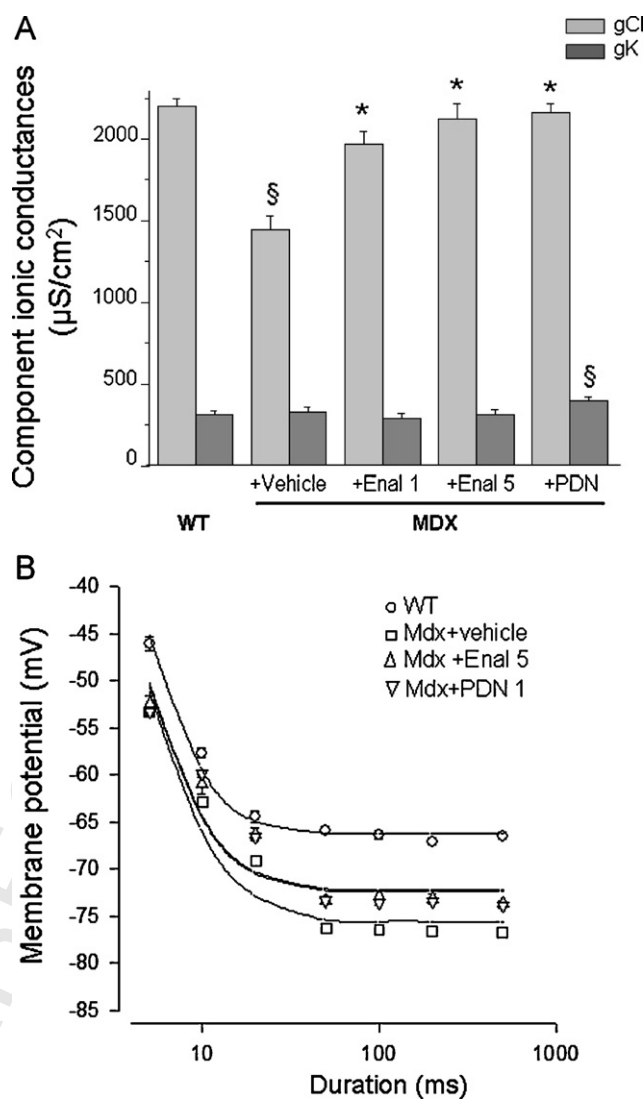


**Fig. 8.** Effect of enalapril treatment on sarcolemmal ionic conductances and mechanical threshold of EDL muscle fibers of mdx mice. (A) Component ionic conductances to chloride (gCl) and potassium (gK) ions of extensor digitorum longus (EDL) muscle fibers of Mdx mice either untreated (+vehicle) or treated with enalapril at 1 mg/kg (Enal 1); enalapril at 5 mg/kg (Enal 5) or  $\alpha$ -methyl prednisolone at 1 mg/kg (PDN). Each column is the mean  $\pm$  S.E.M. from 15 to 30 fibers from 3 to 7 preparations. The ANOVA test for multiple comparison was significant for both gCl ( $F > 16$ ;  $p < 0.0001$ ) and gK ( $F = 3.7$ ;  $p < 0.02$ ). Bonferroni's *t* test is as follows: \*Significantly different with respect to untreated MDX mice ( $p < 0.0001$ ); §Significantly different with respect to WT for either gCl ( $p < 0.0001$ ) or gK ( $p < 0.02$ ). (B) Effect of treatment with enalapril 5 mg/kg (Enal 5) and  $\alpha$ -methyl prednisolone (PDN) on mechanical threshold of Extensor digitorum longus (EDL) muscle fibers. The data, expressed as mean  $\pm$  S.E.M. from 10 to 34 values from 3 to 5 preparations (see also Table 2), show the voltages for fiber contraction (mechanical threshold) at each pulse duration in different experimental conditions and in particular in wildtype (WT, open circles), vehicle-treated mdx mice (Mdx+vehicle, open squares), and PDN (upside-down open triangles) or Enalapril treated (open triangles) mdx mice. For some data point the standard error bar is not visible being smaller than symbol size. The fit of the experimental data lead to the calculation of rheobase voltage values reported in the text.

**Table 3**  
Effect of Enalapril treatment on mechanical threshold of extensor digitorum longus (EDL) muscle fibers of mdx mice.

Experimental conditions	5 ms	10 ms	20 ms	50 ms	100 ms	200 ms	500 ms
WT	-49.0 ± 0.5(10)	-61.9 ± 0.7(12)	-66.7 ± 0.7(11)	-69.7 ± 0.4(14)	-68.6 ± 0.6(15)	-69.8 ± 0.5(14)	-70.5 ± 0.4(16)
Mdx + vehicle	-53.4 ± 0.5(17)	-62.9 ± 0.5(16)	-69.1 ± 0.3(17)	-76.3 ± 0.3(20)	-76.4 ± 0.3(19)	-76.6 ± 0.2(19)	-76.8 ± 0.2(23)
Mdx + Enal 5	-52.5 ± 0.9(16)	-61.0 ± 1.1(15)	-66.3 ± 0.7*(17)	-73.3 ± 0.4*(25)	-72.9 ± 0.5*(21)	-73.2 ± 0.5*(23)	-73.7 ± 0.3*(34)
Mdx + PDN	-53.3 ± 0.4(31)	-59.9 ± 0.3*(29)	-66.6 ± 0.2*(30)	-73.4 ± 0.2*(33)	-73.6 ± 0.2*(33)	-73.4 ± 0.2*(32)	-73.9 ± 0.2*(34)

The columns from left to right are as follows. Experimental conditions, the fibers sampled are from extensor digitorum longus (EDL) muscles from mdx mice untreated (Mdx + vehicle) or treated with the test compounds: enalapril at 5 mg/kg (Enal 5) and  $\alpha$ -methylprednisolone (PDN). For each experimental group are shown the threshold membrane potential values obtained with depolarizing command pulse of duration ranging from 5 up to 500 ms. The values are expressed as mean  $\pm$  S.E.M. from the number of fibers shown in parentheses below each value. For each experimental condition at least 3-5 animals were sampled. In all mdx groups, the threshold values from 50 to 500 ms are significantly different with respect to WT ones. \*Significantly different with respect to Mdx + vehicle group by ANOVA and Bonferroni *t*'test correction ( $p < 0.05$  and less).

from enalapril treated mice (5 mg/kg) and in particular in centronucleated fibers (35% over total positive myofibers); however the quantitative analysis of total reactivity showed that this trend was not statistical significant, again supporting a minor anti-fibrotic effect of enalapril at this pathology stage (Fig. 6, lower panel).

We next evaluated if the improved in vivo performance, the reduction of muscle necrosis and the reduced markers of oxidative stress were paralleled by an amelioration of the biochemical markers of pathology. The high plasma level of creatine kinase (CK) is a clear diagnostic sign of dystrophic muscle damage. None of the treatments exerted significant reduction of plasma CK. Similarly, no significant changes were observed in the plasma level of lactate dehydrogenase (LDH), taken as a marker of contraction-induced metabolic distress (Fig. 7). Then, all the values remained significantly higher than those of wt animals (data not shown).

#### 3.4. Effect of enalapril on functional myofiber parameters

Functional cellular parameters can be taken as biomarkers of muscle state. A specific marker of spontaneous and/or exercise induced myofiber damage is the significant reduction of the macroscopic conductance to chloride ion (gCl). gCl is sensitive to the direct action of pro-inflammatory cytokines; consequently, anti-inflammatory drugs or partial increase in dystrophin level exert protective effects on this cellular index [26,28,29,33]. The treatment with enalapril lead to a significant and dose-dependent increase in gCl values in EDL myofibers. The recovery score for this parameter was 69% and 90% in 1 and 5 mg/kg treated mdx EDL, respectively (Fig. 8A). The effect observed was slightly lower than that observed in PDN-treated EDL muscle (recovery score 95%) thus corroborating that it may be due to the ability of blunting an inflammation-related mechanism. In addition, preliminary results suggest that muscle chloride channels can be a direct target of Ang-II action via activation of an AT1 receptor [35]. A clear trend toward a dose-dependent increment of gCl was also observed in diaphragm as gCl was  $1446 \pm 86 \mu\text{S}/\text{cm}^2$  ( $N/n = 5/43$ );  $1524 \pm 82 \mu\text{S}/\text{cm}^2$  ( $N/n = 4/40$ );  $1632 \pm 125 \mu\text{S}/\text{cm}^2$  ( $N/n = 3/19$ ) in vehicle, 1 mg/kg and 5 mg/kg enalapril-treated, respectively. The less efficacy in diaphragm vs. EDL muscle could be likely related to the possible different mechanism underlying the impairment of the chloride channel in the two muscle types [26,28]. No significant effect of enalapril treatment was observed on potassium conductance (gK) in either EDL muscle (Fig. 8) or diaphragm (data not shown).

The effects of enalapril were also evaluated on the alteration of the voltage threshold for contraction (mechanical threshold, MT), a calcium-dependent electrophysiological index of excitation-contraction (e-c) coupling mechanism [28]. The alteration of this parameter, along with that of cytosolic calcium level, can be fully contrasted by drugs able to directly act on the channels that contribute to the enhanced sarcolemmal permeability in mdx myofibers [19,36]. The threshold potential values of enalapril-

treated EDL mdx fibers were slightly, albeit significantly, shifted toward more positive potentials vs. those of untreated ones, mostly at the long depolarizing steps (from 50 ms ahead) (Table 3). Then, a shift of the strength-duration curve toward more positive potentials was observed in enalapril-treated muscle (Fig. 8B). The rheobase values calculated from the fit were  $-72.2 \pm 1.3$  mV and  $-75.6 \pm 1.24$  mV for enalapril and vehicle-treated muscles, respectively. The difference was not statistically significant ( $t = 1.8$ ;  $p > 0.05$ ). Both values were still highly significantly different with respect to that of wild-type myofibers ( $-66.2 \pm 0.47$  mV;  $p < 0.001$ ). The effect of 5 mg/kg enalapril almost overlapped that observed with PDN and underlined a modest recovery score (around 35%) on the calcium homeostasis. No effect of either drug was observed on the time constant to reach the rheobase (data not shown). The result is in line with the observation that other drugs acting as pure anti-inflammatory compounds do not exert any improvement in calcium homeostasis of mdx myofibers, and suggests that the modest benefit of both enalapril and PDN could be related to the anti-oxidant effects, in relation to the possible cross-talk between ROS and calcium handling mechanisms [20,26,33].

#### 4. Conclusions

ACE inhibitors are a widely used class of drugs for cardiovascular disorders due to their ability to reduce both short and long term effects of Ang II on function and re-modelling of heart and vascular system. Accordingly, ACE inhibitors are already clinically used to contrast cardiomyopathy occurring in Duchenne patients, and data from clinical trials corroborate the ability of these drugs in prolonging survival [8,9]. The establishment of direct beneficial effect of this class of therapeutics at skeletal muscle level in parallel with the clarification of their mechanism of action can further reinforce their clinical use in DMD. In fact, data in the literature support a potential involvement of RAS in muscles of DMD patients, with over-expression of angiotensin converting enzyme and of AT-1 receptor, in parallel with TGF- $\beta$ 1, in regenerating muscle fibers, fibroblasts and inflammatory infiltrates [37]. This is supported by recent evidence of the presence of several components of RAS in myofibers, corroborating an autocrine production of Ang II in skeletal muscle, potentially triggered by mechanical challenge [38], a critical issue for dystrophic muscle. In addition, long term and indirect activation of systemic RAS, such as that consequent to congestive heart failure, also plays a role in skeletal muscle atrophy, through direct action of Ang II in regulating the two ubiquitin ligases atrogenin-1 and muscle ring finger-1 (MuRF-1) [16,39]. Although direct evidence about involvement of RAS in the murine pathology is not available, pre-clinical studies in mdx mice claimed a prominent role of Ang-II-TGF $\beta$ -pathway in late occurring fibrosis and failing regeneration [11]. Our results favor a role of Ang-II in early inflammatory phases of muscular dystrophy, supporting a wider protective role of ACE inhibitors in dystrophic muscle. Mostly, the results of our study evidenced the

ability of enalapril to exert protective effects on mouse strength, while significantly reducing the production of ROS and the activation of NF- $\kappa$ B, pathways that play a key role in muscular dystrophy [18,19,23]. Our results are in line with various evidences showing that Ang-II has pro-inflammatory actions and contributes to insulin resistance in myocytes via ROS-independent and dependent pathways, these latter involving a receptor and NF- $\kappa$ B-mediated activation of NADPH oxidase [17,40,41]. Interestingly, Ang II has been recently claimed to exert a wasting catabolic effect in mouse skeletal muscle via NADPH oxidase derived ROS [42], while losartan protects against disuse atrophy in rodent sarcopenia via a TGF- $\beta$ 1 independent signaling which rather involves the activation of insulin-like growth factor 1 (IGF-1) pathways [43]. Then it is feasible that in dystrophic pathology RAS may contribute to the early inflammatory microenvironment necessary to reinforce the damaging later effects via TGF- $\beta$ 1, meanwhile weakening the IGF-1-dependent regenerative program [12,13,44]. Accordingly, in the present study we found a clear reduction of muscle necrosis by enalapril, with minor, if any, effects on non-muscle tissue, TGF- $\beta$ 1 level and p-Smad 2/3 reactivity, supporting earlier actions vs. the induction of fibrosis. The possibility that enalapril also acts by contrasting functional ischemia cannot be ruled out, although the modest recovery of resistance to exercise does not support this view.

However, in contrast with other anti-inflammatory compounds [26,33], enalapril did not reduce CK and LDH. The lack of effect on CK, also routinely observed in our experimental condition with PDN [27], has also been observed in long-term losartan treated mdx mice [11]. In a strict sense CK level cannot be taken as a reliable outcome measure for therapeutics as it might be influenced by the amount of muscle/animal activity, or to other drug actions at sarcolemmal level.

Then, it is feasible to conclude that Ang II represents an early upstream signals in triggering a chronic inflammatory state and dystrophic muscle damage and its early blockade may help in halting the establishment of auto-reinforcing signals. The results add new evidences about the potential interest of ACE inhibitors for the therapy of DMD patients and support their early use. The PDN-similar profile may corroborate the combined use of the two classes of drugs in DMD patients so to potentiate the beneficial effects at skeletal muscle level, while reducing both spontaneous and PDN-aggravated cardiomyopathy [10].

## Acknowledgement

The financial support of Italian Telethon to the project no. GGP05130 is gratefully acknowledged.

## References

- [1] Grounds MD, Radley HG, Lynch GS, Nagaraju K, De Luca A. Towards developing standard operating procedures for pre-clinical testing in the mdx mouse model of Duchenne muscular dystrophy. *Neurobiol Dis* 2008;31:1-19.
- [2] Willmann R, Possekel S, Dubach-Powell J, Meier T, Ruegg MA. Mammalian animal models for Duchenne muscular dystrophy. *Neuromuscul Disord* 2009;19:241-9.
- [3] Hoffman EP, Dressman D. Molecular pathophysiology and targeted therapeutics for muscular dystrophy. *Trends Pharmacol Sci* 2001;22:465-70.
- [4] Rando TA, Disatnik MH, Yu Y, Franco A. Muscle cells from mdx mice have an increased susceptibility to oxidative stress. *Neuromuscul Disord* 1998;8:14-21.
- [5] Whitehead NP, Yeung EW, Allen DG. Muscle damage in mdx (dystrophic) mice: role of calcium and reactive oxygen species. *Clin Exp Pharmacol Physiol* 2006;33:657-62.
- [6] Bushby K, Straub V. Nonmolecular treatment for muscular dystrophies. *Curr Opin Neurol* 2005;18:511-8.
- [7] Bushby K, Finkel R, Birnkrant DJ, Case LE, Clemens PR, Cripe L, et al. Diagnosis and management of Duchenne muscular dystrophy, part 1: diagnosis, and pharmacological and psychosocial management. *Lancet Neurol* 2010;9:77-93.

- [8] Duboc D, Meune C, Lerebours G, Devaux JY, Vaksman G, Bécane HM. Effect of perindopril on the onset and progression of left ventricular dysfunction in Duchenne muscular dystrophy. *J Am Coll Cardiol* 2005;45:855-7.
- [9] Duboc D, Meune C, Pierre B, Wahbi K, Eymard B, Toutain A, et al. Perindopril preventive treatment on mortality in Duchenne muscular dystrophy: 10 years' follow-up. *Am Heart J* 2007;154:596-602.
- [10] Bauer R, Straub V, Blain A, Bushby K, MacGowan GA. Contrasting effects of steroids and angiotensin-converting-enzyme inhibitors in a mouse model of dystrophin-deficient cardiomyopathy. *Eur J Heart Fail* 2009;11:463-71.
- [11] Cohn RD, van Erp C, Habashi JP, Soleimani AA, Klein EC, Lisi MT, et al. type 1 receptor blockade attenuates TGF-beta-induced failure of muscle regeneration in multiple myopathic states. *Nat Med* 2007;13:204-10.
- [12] Berk BC, Fujiwara K, Lehoux S. ECM remodeling in hypertensive heart disease. *J Clin Invest* 2007;117:568-75.
- [13] Wynn TA. Cellular and molecular mechanisms of fibrosis. *J Pathol* 2008;214:199-210.
- [14] Martin MM, Buckenberger JA, Jiang J, Malana GE, Knoell DL, Feldman DS, et al. TGF-beta1 stimulates human AT1 receptor expression in lung fibroblasts by cross talk between the Smad, p38 MAPK, JNK, and PI3K signaling pathways. *Am J Physiol Lung Cell Mol Physiol* 2007;293:L790-9.
- [15] Gazzero E, Assereto S, Bonetto A, Sotgia F, Scarfi S, Pistorio A, et al. Therapeutic potential of proteasome inhibition in Duchenne and Becker muscular dystrophies. *Am J Pathol* 2010;176:1863-77.
- [16] Russell ST, Wyke SM, Tisdale MJ. Mechanism of induction of muscle protein degradation by angiotensin II. *Cell Signal* 2006;18:1087-96.
- [17] Wei Y, Sowers JR, Clark SE, Li W, Ferrario CM, Stump CS. Angiotensin II-induced skeletal muscle insulin resistance mediated by NF-kappaB activation via NADPH oxidase. *Am J Physiol Endocrinol Metab* 2008;294:E345-351.
- [18] Arthur PG, Grounds MD, Shavlakadze T. Oxidative stress as a therapeutic target during muscle wasting: considering the complex interactions. *Curr Opin Clin Nutr Metab Care* 2008;11:408-16.
- [19] Burdi R, Rolland JF, Fraysse B, Litvinova K, Cozzoli A, Giannuzzi V, et al. Multiple pathological events in exercised dystrophic mdx mice are targeted by pentoxifylline: outcome of a large array of in vivo and ex vivo tests. *J Appl Physiol* 2009;106:1311-24.
- [20] Shkryl VM, Martins AS, Ullrich ND, Nowycky MC, Niggli E, Shirokova N. Reciprocal amplification of ROS and Ca(2+) signals in stressed mdx dystrophic skeletal muscle fibers. *Pflugers Arch* 2009;458:915-28.
- [21] Spurney CF, Knoblich S, Pistilli EE, Nagaraju K, Martin GR, Hoffman EP. Dystrophin-deficient cardiomyopathy in mouse: expression of Nox4 and Lox are associated with fibrosis and altered functional parameters in the heart. *Neuromuscul Disord* 2008;18:371-81.
- [22] Williams IA, Allen DG. The role of reactive oxygen species in the hearts of dystrophin-deficient mdx mice. *Am J Physiol Heart Circ Physiol* 2007;293:H1969-1977.
- [23] Acharyya S, Villalta SA, Bakkar N, Bupha-Intr T, Janssen PM, Carathers M, et al. Interplay of IKK/NF-kappaB signaling in macrophages and myofibers promotes muscle degeneration in Duchenne muscular dystrophy. *J Clin Invest* 2007;117:889-901.
- [24] Messina S, Altavilla D, Aguenouz M, Seminara P, Minutoli L, Monici MC, et al. Lipid peroxidation inhibition blunts nuclear factor-kappaB activation, reduces skeletal muscle degeneration, and enhances muscle function in mdx mice. *Am J Pathol* 2006;168:918-26.
- [25] Wang P, Fedoruk MN, Rupert JL. Keeping pace with ACE: are ACE inhibitors and angiotensin II type 1 receptor antagonists potential doping agents? *Sports Med* 2008;38:1065-79.
- [26] De Luca A, Nico B, Liantonio A, Didonna MP, Fraysse B, Pierno S, et al. A multidisciplinary evaluation of the effectiveness of cyclosporine A in dystrophic mdx mice. *Am J Pathol* 2005;166:477-89.
- [27] Cozzoli A, Rolland JF, Capogrosso RF, Splendorio VT, Longo V, Simonetti S, et al. Evaluation of potential synergistic action of a combined treatment with alpha-methyl-prednisolone and taurine on the mdx mouse model of Duchenne muscular dystrophy. *Neuropathol Appl Neurobiol* 2011;37:243-56.
- [28] De Luca A, Pierno S, Liantonio A, Cetrone M, Camerino C, Fraysse B, et al. Enhanced dystrophic progression in mdx mice by exercise and beneficial effects of taurine and insulin-like growth factor-1. *J Pharmacol Exp Ther* 2003;304:453-63.
- [29] De Luca A, Nico B, Rolland JF, Cozzoli A, Burdi R, Mangieri D, et al. Gentamicin treatment in exercised mdx mice: identification of dystrophin-sensitive pathways and evaluation of efficacy in work-loaded dystrophic muscle. *Neurobiol Dis* 2008;32:243-53.
- [30] Ortiz LA, Champion HC, Lasky JA, Gambelli F, Gozal E, Hoyle GW, et al. Enalapril protects mice from pulmonary hypertension by inhibiting TNF-mediated activation of NF-kappaB and AP-1. *Am J Physiol Lung Cell Mol Physiol* 2002;282:L1209-21.
- [31] Reagan-Shaw S, Nihal M, Ahmad N. Dose translation from animal to human studies revisited. *FASEB J* 2008;22:659-61.
- [32] Simolin MA, Pedersen TX, Bro S, Mäyränpää MI, Helske S, Nielsen LB, et al. ACE inhibition attenuates uremia-induced aortic valve thickening in a novel mouse model. *BMC Cardiovasc Disord* 2009;3:9-10.
- [33] Pierno S, Nico B, Burdi R, Liantonio A, Didonna MP, Cippone V, et al. Role of TNF-alpha, but not of COX-2 derived eicosanoids, on functional and morphological indices of dystrophic progression in mdx mice: a pharmacological approach. *Neuropathol Appl Neurobiol* 2007;33:344-59.

- 674 [34] Kobayashi YM, Rader EP, Crawford RW, Iyengar NK, Thedens DR, Faulkner JA, 691  
675 et al. Sarcolemma-localized nNOS is required to maintain activity after mild 692  
676 exercise. *Nature* 2008;456:511-5. 693
- 677 [35] Cozzoli A, Pierno S, Conte Camerino D, De Luca A. Skeletal muscle chloride 694  
678 channel, a biophysical sensor of dystrophic progression in mdx mouse, is a 695  
679 potential target of pro-inflammatory mediators. *Biophys J* 2009;96:469a-70a. 696
- 680 [36] Rolland JF, De Luca A, Burdi R, Andreetta F, Confalonieri P, Conte Camerino D. 697  
681 Overactivity of exercise-sensitive cation channels and their impaired modulation 698  
682 by IGF-1 in mdx native muscle fibers: beneficial effect of pentoxifylline. 699  
683 *Neurobiol Dis* 2006;24:466-74. 700
- 684 [37] Sun G, Haginoya K, Dai H, Chiba Y, Uematsu M, Hino-Fukuyo N, et al. Intramuscular 701  
685 renin-angiotensin system is activated in human muscular dystrophy. *J 702*  
686 *Neurol Sci* 2009;280:40-8. 703
- 687 [38] Johnston AP, Baker J, De Lisio M, Parise G. Skeletal muscle myoblasts possess 704  
688 a stretch-responsive local angiotensin signalling system. *J Renin Angiotensin 705*  
689 *Aldosterone Syst* 2010 [Epub ahead of print]. 706
- 690 [39] Yoshida T, Semprun-Prieto L, Sukhanov S, Delafontaine P. IGF-1 prevents ANG 707  
II-induced skeletal muscle atrophy via Akt- and Foxo-dependent inhibition 708  
of the ubiquitin ligase atrogin-1 expression. *Am J Physiol Heart Circ Physiol* 2010;298:H1565-1570.
- [40] Seshiah PN, Weber DS, Rocic P, Valppu L, Taniyama Y, Griendling KK. 691  
Angiotensin II stimulation of NAD(P)H oxidase activity: upstream mediators. 692  
*Circ Res* 2002;91:406-13. 693
- [41] White CN, Figtree GA, Liu CC, Garcia A, Hamilton EJ, Chia KK, et al. Angiotensin 694  
II inhibits the Na<sup>+</sup>-K<sup>+</sup> pump via PKC-dependent activation of NADPH oxidase. 695  
*Am J Physiol Cell Physiol* 2009;296:C693-700. 696
- [42] Semprun-Prieto LC, Sukhanov S, Yoshida T, Rezk BM, Gonzalez-Villalobos RA, 697  
Vaughn C, et al. Angiotensin II induced catabolic effect and muscle atrophy are 698  
redox dependent. *Biochem Biophys Res Commun* 2011. May 6 [Epub ahead of 699  
print]. 700
- [43] Burks TN, Andres-Mateos E, Marx R, Mejias R, Van Erp C, Simmers JL, et al. Losar- 701  
tan restores skeletal muscle remodeling and protects against disuse atrophy in 702  
sarcopenia. *Sci Transl Med* 2011;3(82):ra37. 703
- [44] Lanz TV, Ding Z, Ho PP, Luo J, Agrawal AN, Srinagesh H, et al. Angiotensin 704  
II sustains brain inflammation in mice via TGF-beta. *J Clin Invest* 2010;120: 705  
2782-94. 706  
707  
708

UNCORRECTED PROOF